Graphene oxide induced pH alteration, iron overload and subsequent oxidative damage in rice (Oryza. sativa L.)

Zhang, Peng; Guo, Zhiling; Luo, Wenhe; Monikh, Fazel Abdolahpur; Xie, Changjian; Valsami-Jones, Eugenia; Lynch, Iseult; Zhang, Zhiyong

DOI:
10.1021/acs.est.9b05794

Contaminants in Aquatic and Terrestrial Environments

Graphene Oxide Induced pH Alteration, Iron Overload and Subsequent Oxidative Damage in Rice (Oryza. sativa L.): A New Mechanism of Nanomaterial Phytotoxicity

Peng Zhang, Zhiling Guo, Wenhe Luo, Fazel Abdolahpur Monikh, Changjian Xie, Eugenia Valsami-Jones, Iseult Lynch, and Zhiyong Zhang

Environ. Sci. Technol., **Just Accepted Manuscript** • DOI: 10.1021/acs.est.9b05794 • Publication Date (Web): 21 Feb 2020

Graphene Oxide Induced pH Alteration, Iron Overload and Subsequent Oxidative Damage in Rice (*Oryza. sativa* L.): A New Mechanism of Nanomaterial Phytotoxicity

Peng Zhang,[a,b,*] Zhiling Guo,[b] Wenhe Luo,[a] Fazel Abdolahpur Monikh,[c] Changjian Xie,[a] Eugenia Valsami-Jones,[b] Iseult Lynch,[b] Zhiyong Zhang[a,*]

[a] *Key Laboratory for Biological Effects of Nanomaterials and Nanosafety, Institute of High Energy Physics, Chinese Academy of Sciences, Beijing 100049, China.*

[b] *School of Geography, Earth and Environmental Science, University of Birmingham, Edgbaston, B15 2TT Birmingham, UK.*

[c] *Institute of Environmental Sciences (CML), Leiden University, 2300, RA, Leiden, Netherlands*

***Corresponding Author.**

E-mail address: pengzhang@ihep.ac.cn (P. Zhang); zhangzhy@ihep.ac.cn (Z.Y. Zhang)

ABSTRACT

The mechanism of graphene-based nanomaterial (GBM) induced phytotoxicity and its association with the GBM physicochemical properties are not yet fully understood. The present study compared the effects of graphene oxide (GO) and reduced GO(rGO) on rice seedling growth under hydroponic condition for 3 weeks. GO at 100 and 250 mg/L reduced shoot biomass (by 25% and 34%, respectively) and shoot elongation (by 17% and 43%, respectively), and caused oxidative damage, while rGO exhibited no overt effect except for the enhancement of the antioxidant enzyme activities, suggesting that surface oxygen content is a critical factor affecting the biological impacts of GBMs. GO treatments (100 mg/L and 250 mg/L) enhanced the iron (Fe) translocation and caused excessive Fe accumulation in shoots (2.2 and 3.6 times higher than control), which was found to be the main reason for the oxidative damage in shoots. GO-induced acidification of the nutrient solution was the main driver for the Fe overload in plants. In addition to the antioxidant regulators, the plants triggered other pathways to defend against the Fe toxicity, *via* downregulation of the Fe transport associated metabolites (mainly coumarins and flavonoids). Plant root exudates facilitated the reduction of toxic GO to non-toxic rGO, acting as another route for plant adaption to GO induced phytotoxicity. This study provides new insights into the mechanism of the phytotoxicity of GBMs. It also provides implications for agricultural application of GBM that the impacts of GBMs on the uptake of multiple nutrients in plants should be assessed simultaneously and reduced forms of GBMs are preferential to avoid toxicity.

TABLE OF CONTENTS

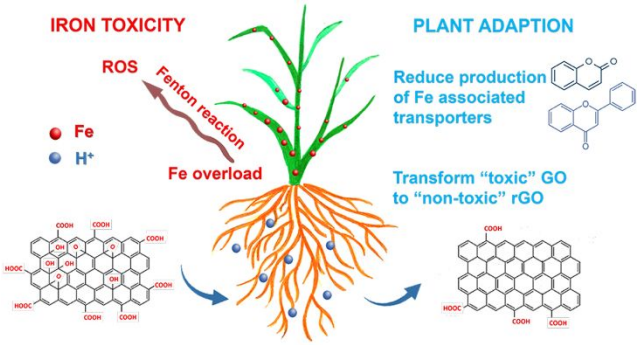

INTRODUCTION

Graphene is a two-dimensional carbon-based nanomaterial composed of a single layer of sp^2 hybridized carbon atoms.[1] It is considered one of the most promising engineered nanomaterials (ENM) with the potential to be used in various sectors such as electronics, medical, energy and environment,[2-4] due to its unique electronic, thermal and mechanical properties. The increasing production and use of graphene-based materials (GBMs) will inevitably increase the likelihood of their release into the environment, and thus their potential adverse impacts on environmental and human safety need to be fully assessed.[5]

There have been extensive studies regarding the toxicity of GBMs on cells and microorganisms,[6, 7] while knowledge of the potential impacts of GBMs on the growth of higher plants is still lacking. There is concern that GBMs may affect plant growth and /or accumulate in crops or vegetables,[8] causing potential risks to human health. Recent studies showed that GBMs have the potential to be used as a carrier for fertilizers to enable slow release of the nutrients and thus enhance the nutrient use efficiency by plants;[9-11] however, such applications in real agriculture are not currently pursued partially due to the concerns over the potential adverse impacts of GBMs on the overall agricultural ecosystem, including soil functioning (e.g., bacterial community, enzyme activity),[12-14] the potential trophic transfer of GBMs[15] and cummulative effects of GBMs after repeated application and over multiple growing seasons.

Overt toxicity of GBMs to plant such as inhibition of biomass production, shoot or root elongation have been reported at high exposure concentrations.[16, 17] However, a number of studies also reported that GBMs induced physiological alterations (e.g., hormone levels, nutrient uptake)[17, 18] or oxidative stress (e.g., enhanced antioxidant enzymatic activities, lipid peroxidation, or H_2O_2 over-accumulation)[16, 19] even at environmentally relevant concentrations (0.01~1mg/L),[20] suggesting that subtle physiological processes are more sensitive indices than apparent toxicity indices (e.g., biomass, root/shoot length) for evaluating the phytotoxicity of GBMs.[21] In addition to the negative effects, positive effects resulting from exposure to GBMs on plant growth are also reported. For example, hydrated graphene ribbons promoted the germination of wheat seeds, upregulated carbohydrate, amino acids and fatty acids metabolism

during the germination and enhanced the tolerance of seeds to oxidative stress.[22] Due to the hydrophilic nature of GO, it can act as a water transporter to promote the seed germination.[23]

There are several reasons that may contribute to the inconsistent reports regarding the phytotoxicity of GBMs. Firstly, phytotoxicity of ENMs are species-dependent,[24] cross-species comparison is not always suitable. Secondly, using different culture media such as soil,[23] agar[25] and hydroponic solutions[19] which have different compositions, can affect the behaviour, fate and toxicity of the GBMs. GBM in soil and agar media usually have low mobility and accessibility to plants, thereby lowering their impacts on plant growth found in such media when compared with those observed in hydroponic media. However, this might be not always true. For example, CeO_2 ENMs were reported to be more toxic to *Lactuca* plants in agar medium than in water, which is due to that *Lactuca* plants are more sensitive in agar than in water to the toxicity of Ce^{3+} ions released from CeO_2 ENMs.[26] Lastly, the physicochemical properties of the GBMs used in the previous studies are very diverse and are not fully described in many cases. In reviewing the studies on the effects of GBMs on higher plants (Table S1), more than half of the papers considered did not provide sufficient characterization data including lateral size, thickness and surface oxygen content, which are critical characteristics determining the biological effects of GBMs.[5] Where provided, the given properties were very varied: the lateral size used in these studies ranged from 30 nm to 6.5 μm, the layer thickness ranged from 0.3 nm to 3.5 nm, and the surface oxygen contents ranged from 3.51% to 38.8%. Clearly, more studies are required to provide sufficient data for cross comparison and elucidating the mechanism(s) of action of GBMs, and to determine the ranges of GBMs' properties that can be used safely to enhance plant growth and /or soil quality and nutrient cycling.

Common forms of graphene, including graphene (G), graphene oxide (GO) and reduced graphene oxide (rGO), are distinct in their surface oxygen contents. GO is the oxidized form of graphene, which contains abundant functional groups including carboxyl, hydroxyl, epoxy, and carbonyl groups.[27] These functional groups endow GO with high water dispersity and can be used for further functionalization of GO for different applications.[3] Previous studies have suggested that GO and rGO have distinct antibacterial activities,[28] which is attributed to the

different modes of interaction of GO and rGO with cell membranes. We hypothesize that comparing the phytotoxicity of GO and rGO, which is yet to be studied, will allow acquisition of a mechanistic understanding of the actions of GBMs in plants. To do so, we investigated the impacts of GO and rGO on the growth of rice plants. Oxidative stress, perturbation of the uptake of macro- and micro- elements in plants, metabolic alteration and the transformation of GO and rGO in rice plants were compared to explore the mechanisms of the interaction of GO and rGO with plants and their consequences for plant health.

2. MATERIALS AND METHODS

2.1. Chemicals and Seeds

GO and rGO were purchased from Chengdu Organic Chemicals Co. Ltd (Chengdu, China). Morphology, lateral size, height, chemical structure, Zeta potential and hydrodynamic sizes of GO and rGO were characterized, details of which are described in the Supporting Information (Section 1). All other commercial chemicals were purchased from Sinopharm Chemical Reagent Co., Ltd (Shanghai, China). Rice (*Oryza. sativa* L.) seeds were purchased from the Chinese Academy of Agricultural Sciences.

2.2. Plant Culture and Exposure

Rice seeds were germinated in the dark for 5 days after sterilization with 10% NaClO . Uniform seedlings were then selected and each seedling was anchored by a plastic foam with a hole and transferred into a 250 mL beaker containing 100 mL of modified 1/4 strength Hoagland solution. All the beakers were wrapped with black plastic bags to simulate the dark environment in soil. Six replicates were set for each treatment. The seedlings were allowed to grow in a growth chamber (PRX-450C, Saifu, China) with a day/night temperature of 28 ^{o}C /20 ^{o}C, day/night humidity of 50%/70% and a 14 h photoperiod for 10 days before treatment. GO and rGO were then added into freshly prepared nutrient solution to obtain suspensions with concentrations of 5, 50, 100 and 250 mg/L followed by ultrasonic pre-treatment for 10 min. The seedlings were then exposed to the GO and rGO suspensions and allowed to grow for three

weeks. The suspensions were replenished to 100 mL with fresh nutrient solution every two days.

2.3. Biomass Production, Seedling Length and Nutrient Content

After three weeks of exposure to the GBMs, rice seedlings were gently lifted from the suspensions, and the roots were rinsed with deionized water repeatedly. GO and rGO that were attached to the roots were rinsed off with deionized water for further analysis. Residual GO and rGO in the beakers were also collected for characterization. The roots and shoots were separated and blotted with clean tissues, and the fresh weights were measured immediately. The seedlings were then lyophilized, and the dry weights of the roots and shoots were measured. To quantify the nutrient content (Fe, Cu, Mn, Zn, K, Ca, Mg, P) in plants, dried roots and shoots were ground into fine powders and digested with a 3:1 mixture of HNO_3 and H_2O_2 on a heating plate (80^{o}C for 1 h, 120 ^{o}C for 3 h, and 160 ^{o}C for 0.5 h). Elemental concentrations in the digestion solution were then analyzed by inductively coupled plasma optical emission spectroscopy (ICP-OES, Thermo, USA). Multi-element standard solutions (0.5~50 mg/L) containing all the selected elements were used for external calibration. Blanks were analysed between every six samples. Spiking recovery experiments and analysis of certified reference material (GBW 07602 Bush Branches and Leaves) were performed for analytical method validation. Recoveries and detection limits for all the elements are reported in Table S2.

2.4. Stress Response of Rice to GO and rGO

Fresh roots and shoots were excised, homogenized with cold PBS (50 mM, pH 7.8), and centrifuged at 10,000 g and 4 °C for 10 min. The supernatants were collected for analyses of superoxide dismutase (SOD) and peroxidase (POD) activities and malondialdehyde (MDA) content using assay kits purchased from Nanjing Jiancheng Bioengineering Institute (Nanjing, China). Reactive oxygen species (ROS) accumulation in roots and leaves was examined by a DCFH-DA staining method. Fresh leaves and roots were excised and incubated in DCFH-DA (10 mM in PBS) for 2 h followed by rinsing with PBS three times. ROS accumulation was imaged on a fluorescence microscope (Olympus IX70) with an ex/em of 485nm/522nm. QA/QC for the assays are described in Section 1, SI.

2.5. Characterization of GO and rGO After Interaction with Plants

After harvesting of the plants, GO and rGO that were attached to the root surface were washed off from the roots using ddH_2O (named "GO-W and rGO-W) and collected by centrifugation (10,000 g, 30 min). The pellets were then rinsed with hydrochloric acid and ethanol repeatedly to remove salts and organic components.[29] The obtained pellets were then freeze-dried for analysis. The residual solutions in the beaker after removal of the plants were also collected and rinsed by the same procedure described above. GO and rGO incubated in nutrient solution for three weeks without the presence of plants were also collected for comparison. All the materials described above (washed and residual) were analyzed by Raman (Horiba Scientific, Japan), FTIR (Bruker Tensor 27 spectrometer, Germany), UV-vis spectroscopy (Purkinje General, Beijing), and XPS (ESCALAB 250Xi, Thermo Scientific, USA). To analyze the GO and rGO on the root surface *in situ*, fresh root apexes were freeze-dried and analysed on a Raman spectrometer (Horiba Scientific, Japan). Fresh root apexes were also excised, fixed and sectioned for TEM observation (see details in the Supporting Information).

2.6. Xylem Sap Collection and Fe concentration Analysis

Rice seedlings were exposed to GO and rGO for 3 weeks as per the exposure procedure in section 2.2 and then cut off at 2 cm above the root-shoot interface. The cut surface of the shoot was cleaned with DI water and then a silicon tube was fit to the stump (Fig. S1). The xylem sap was collected after 24 h with a pipette and digested in HNO_3 (70%). Iron concentrations in the xylem saps were analysed by ICP-OES (Thermo, USA).

2.7. Metabolomics analysis of rice leaves

The fresh rice leaves were thoroughly rinsed with ddH_2O after harvest and ground into powder in liquid nitrogen. For each sample, 100 mg powder was transferred to a 1.5 mL Eppendorf tube and mixed with 2 mL methanol by vortexing vigorously. Samples were ultrasonicated for 1 hour min at 4°C and dried under a stream of N_2. Then, 500 μL of cold methanol was added to each sample. The samples were mixed by vigorous vortexing followed by centrifugation at 12,000 rpm for 10 min at 4°C. A 300 μL aliquot of supernatant was then transferred into a glass

sampling vial for analysis. Samples were then analysed by liquid chromatography-tandem MS (LC-MS/MS). Details of the measurement and data analysis are described in the Supporting Information.

2.8. Data processing

All statistical data were presented as means ± standard deviation. Statistical analysis was performed using IBM SPSS Statistics 19. One way ANOVA with a Tukey's test was applied after testing the data for normality and homoscedasticity, to analyse whether there were significant differences for the data of biomass, root length, stress response, and elemental concentrations between exposure conditions. $P < 0.05$ was considered statistically significant.

3. RESULTS AND DISCUSSION

3.1. Characterization of GO and rGO

SEM images show the morphology of GO and rGO sheets (Fig. 1A and 1B). The average sizes of GO (0.089 ± 0.023 μm) and rGO (0.078 ± 0.034 μm) are not significantly different (Fig. 1C and 1D). The size distributions are shown in Fig. S2. AFM height profiles show that GO and rGO sheets have a thickness of 0.78 ± 0.26 and 0.44 ± 0.23 nm, respectively. FTIR spectra confirm that GO has a significantly higher amount of oxygen-containing groups (O-H group at 3400 cm^{-1}, C=O group at 1726 cm^{-1}, C-O group at 1416 and 1052 cm^{-1}) than rGO. XPS survey analysis shows 34.6% and 7.8% of atomic oxygen in GO and rGO, respectively (Fig. S3). Peak fitting analysis of high-resolution XPS spectra suggests that the amount of oxygen containing groups in GO and rGO are 61% and 23%, respectively. DLS analysis suggests that rGO shows a positive charge in both water and nutrient solution, while GO is negatively charged (Table S3). The hydrodynamic diameters of GO and rGO were larger in nutrient solution (1398 ± 347 nm and 1599 ± 368 nm) than in deionized water (1194 ± 123 nm and 865 ± 98 nm), indicating agglomeration of GO and rGO in nutrient solution, and the sizes of GO and rGO in nutrient solution were similar. The high salinity of the nutrient solution contributed to the compression of the double electric layer on the surface of nanomaterials and subsequent aggregation.[30]

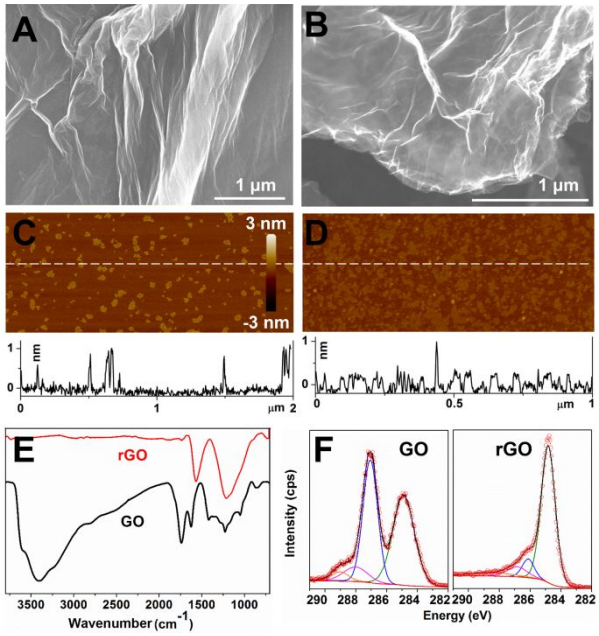

Fig. 1. Characterization of GO and rGO. SEM images of GO (A) and rGO (B); AFM images and height profiles of GO (C) and rGO (D); FTIR spectra of GO and rGO (E); XPS spectra of GO and rGO (F).

3.2. GO and rGO showed distinct effects on rice seedling growth

As shown in Fig. 2, GO and rGO showed distinct impacts on the seedling growth of rice plants. GO showed no effect on root elongation after three weeks of dosing, but significantly reduced the shoot length by 11% at 100 mg/L and by 40% at 250 mg/L (Fig. 2A). GO at 100 mg/L and 250 mg/L also reduced the fresh biomass of both roots and shoots (Fig. 2C), and the dry weight of shoots at 100 mg/L and 250 mg/L (Fig. 2E). In contrast, rGO showed no effect on seedling elongation and biomass production at all concentrations (Fig. 2B, 2D and 2F).

Since the lateral size and hydrodynamic size of GO and rGO are not significantly different, they are not related to the different toxicity between GO and rGO. The thicknesses of GO and rGO are slightly different. It has been reported that increasing the thickness would decrease the sharpness of the edge thus weakening the "nanoknife" effect,[31] that is, GO with a bigger thickness should show lower effects on plant growths than rGO. However, our result is the

opposite, suggesting that thickness is also not a determining factor. These indicate that phytotoxicity of GBMs is mainly dependent on their surface oxygen content.

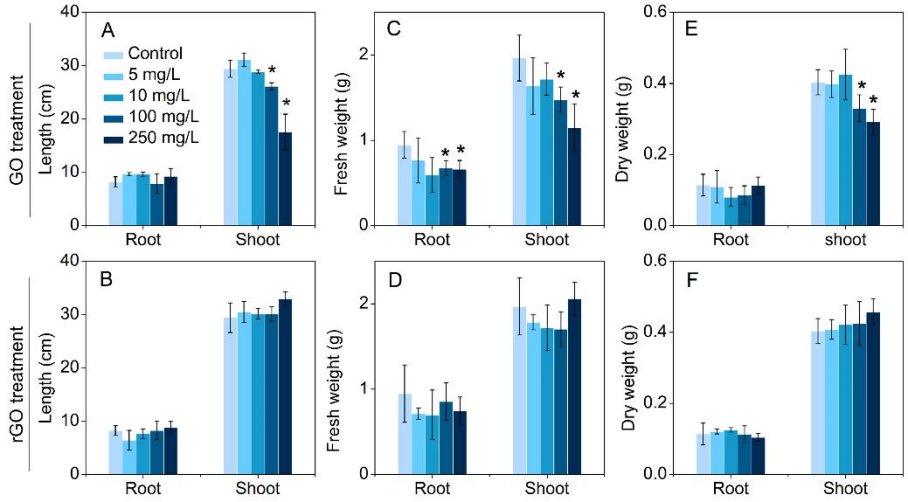

Fig. 2. Seedling lengths (A and B), fresh weights (C and D), and dry weights (E and F) of rice seedlings after exposure to different concentrations of GO and rGO for 3 weeks. Top row shows GO treatments, bottow row shows rGO treatments. * indicates a significant difference compared with control at $P < 0.05$.

3.3. Oxidative stress responses induced by GO and rGO

To further explore the underlying mechanisms of the different responses of rice seedlings and plants to GO and rGO, we examined the oxidative stress responses of rice seedlings to GO and rGO exposure (Fig. 3). The activities of antioxidant enzymes including SOD (Fig. 3A) and POD (Fig. 3B) in shoots following GO treatment were significantly enhanced at 100 mg/L and 250 mg/L whilst the MDA contents in shoots increased by 37% and 70% (Fig. 3C), respectively. No obvious changes of SOD, POD and MDA were observed in roots. In rGO treatments, SOD and POD activity only increased at the highest exposure concentration (250 mg/L) (Fig. 3D and 3E), and there was no alteration of MDA content in either roots or shoots (Fig. 3F). Significant overproduction of ROS was found in shoots with GO treatment while no obvious change was found with rGO treatment (Fig. S4). The enhanced activities of antioxidant enzymes represents a defence mechanism of plants against ambient stress. Both GO an rGO triggered the stress

response of plants, with the enzymatic antioxidant system failing to protect the plants against the GO exposure, with the evidence showing that ROS and MDA over accumulated in GO-exposed plants. Notably, the most overt over accumulation of MDA and ROS in response to GO treatment was found in shoots rather than roots. A similar phenomenon was also reported with maize plants where leaves were more sensitive than roots to the oxidative stress induced by sulfonated graphene;[32] the MDA content in roots was increased only by the highest GO concentration (500 mg/L) while that in leaves was enhanced by GO concentrations ranging from 100 ~ 500 mg/L. The underlying mechanism was explored in the following studies.

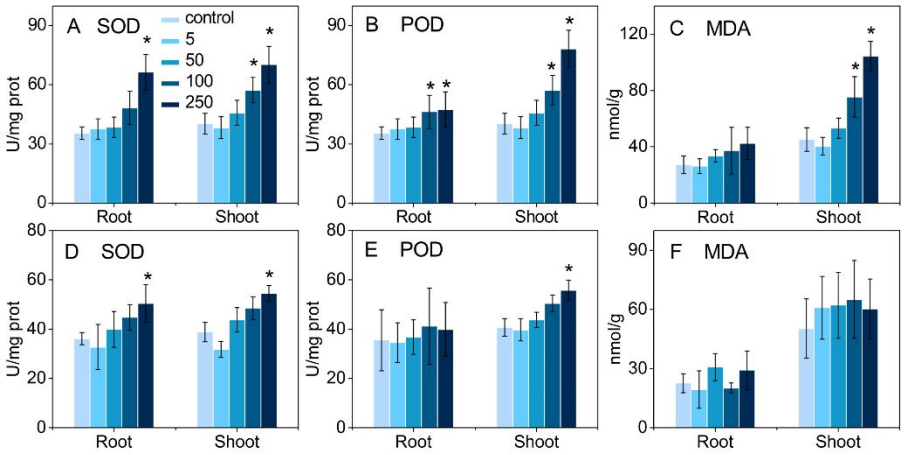

Fig. 3. SOD (A and D) and POD (B and E) activities, and MDA (C and F) contents in rice after exposure to GO and rGO for 3 weeks. Top row: GO treatments, bottom row: rGO treatments. * indicates significant difference compared with control at $P < 0.05$.

3.4. Alteration of the uptake of macro- and micro- elements in plants

To further examine the impact of GO and rGO on plant growth, we measured the uptake of several key nutrients that are essential for plant growth. rGO decreased the Cu level in plant tissues at 50 mg/L but showed no effects on the level of other elements (Fig. S5); however, GO induced alteration of the levels of several elements including P and Fe in shoots and Fe and Zn in roots (Fig. 4). Surprisingly, the Fe level in shoot (415 mg/kg) treated with 250 mg/L of GO was enhanced by 3.6 times as compared with that in the control plants (90 mg/kg). Rice plants usually maintain 60~300 mg/kg of Fe; when the Fe content exceeds 400 mg/kg the plant will

experience toxicity due to Fe overload.[33] The excessive Fe is translocated upwards and accumulated in leaves, impairing the physiological processes of plants by generating ROS via the Haber-Weiss or Fenton reactions.[34] In our study, the total Fe content in the GO-exposed plants was not significantly changed (Fig. S6A); however, the translocation of Fe from root to shoot was greatly enhanced (Fig. S6B). The Fe level in shoots was increased up to 415 mg/kg by the 250 mg/L GO treatment, which is correlated with the over accumulation of ROS and altered antioxidant enzymatic activities in plant leaves. These results suggested that GO induced Fe overload and consequent oxidative stress in leaves is one possible mechanism causing the phytotoxicity observed. The increased P level (Fig. 4A) was unlikely to be the driver of the toxicity because the highest P level in the shoot (9.5 mg/g) was still below the concentration (>13 mg/g) at which P may become toxic to gramineous plants.[35] Additionally, the toxicity in shoots occurred at 100 mg/L when there is no change of P levels, suggesting that P was not necessary for the occurrence of the toxicity.

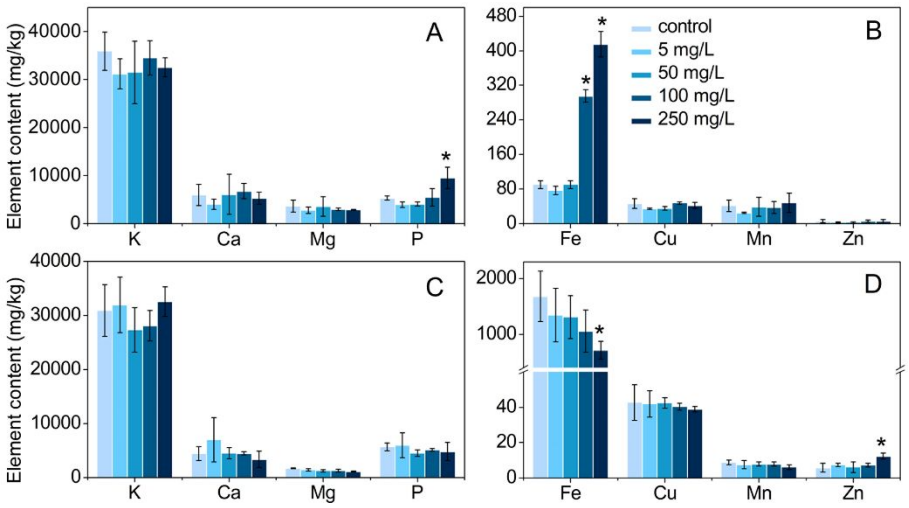

Fig. 4. Macronutrient and micronutrient contents in shoots (A and B) and roots (C and D) of plants after exposure to different concentrations of GO for 3 weeks. * indicates significant difference compared with control at $P < 0.05$.

3.5. Iron overload contributes more than GO *per se* to the GO induced phytotoxicity

Since both GO *per se* and Fe overload may induce oxidative stress in plants, a follow-up question is to understand the contributions of GO and Fe overload to the induced oxidative stress and phytotoxicity. In our study, the oxidative stress, lipid peroxidation and overt phytotoxicity (reduction of biomass and seedling length) were found for leaves rather than roots; this pattern is similar with that found in Fe overloaded plants rather than graphene or other ENM treated plants. For example, it was reported that excessive $FeSO_4$ treatment enhanced the MDA content in rice leaves by 134% while having no effect on the MDA levels in roots.[36] While for ENMs, the roots are usually more sensitive than the leaves to ENM-induced toxicity, which might be due to the fact that most of the ENMs are adsorbed onto the root surface while the upward translocation of ENMs is limited.[37]

Therefore, we deduced that excessive Fe uptake might be the main contributor to the toxicity found in this study rather than GO *per se*. To prove this hypothesis, we added an excessive amount of Fe (4 mM $FeSO_4$) to the 50 mg/L GO suspension and examined the rice seedlings growth. As compared with GO treatment alone, the dry weight of leaves was reduced by 27% (Fig. 5A) and the MDA content in leaves was upregulated by 46% (Fig. 5B) after exposure to GO+$FeSO_4$, which are correlated with a significantly enhanced Fe level in leaves (Fig. 5C). These results suggest that Fe overload contributed more than GO *per se* to the oxidative stress and subsequent toxicity in rice plants, although the effects of GO and rGO cannot be simply ignored since GO and rGO *per se* may generate ROS.[38]

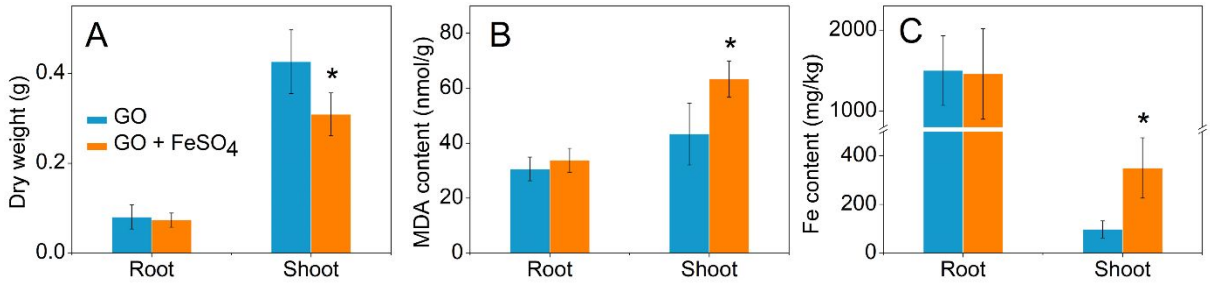

Fig. 5. Dry weight (A), MDA content (B) and Fe content (C) in rice plants after exposure to GO (50 mg/L) and a mixture of GO (50 mg/L) and $FeSO_4$ (4 mM) for 3 weeks. * indicates significant difference compared with GO treatment at $P < 0.05$.

3.6. Mechanisms involved in the overload of Fe in leaves

Under anaerobic conditions, e.g. in paddy fields, Fe usually exists in the form of Fe^{2+} which is bioavailable for plant uptake. To avoid over accumulation of Fe, rice roots can release oxygen and oxidase to oxidize the Fe^{2+} to Fe^{3+}, which precipitates to form a coating on the roots named "Fe plaque".[33] The Fe plaque can prevent not only the uptake of excessive Fe^{2+} but also the entry of toxic heavy metals into plants. However, a decrease of pH can significantly promote the reduction of insoluble Fe^{3+} to Fe^{2+} that eventually leads to Fe toxicity, which affects a significant proportion of rice fields in many developing countries.[33]

The pH mediated Fe uptake not only applies for plants cultured in soil but also applies for hydroponic culture. It was also reported that low pH can significantly promote Fe^{2+} uptake by plants.[39] We found that GO acidified the nutrient solution while rGO didn't change the pH significantly (Fig. 6A). The pH of the GO suspensions decreased with increasing GO concentration. The pH values for 100 mg/L and 250 mg/L of GO in NS are 3.95 and 3.32, respectively, which are much lower than that of the normal NS (pH 5.5). The low pH itself was unlikely the main reason for the toxicity based on two reasons: 1) Rice is relatively tolerant of acidic conditions. Previous studies showed that rice can grow normally at pHs as low as 3.4, but the growth can be greatly impaired if Fe contents in the soil increased.[40] 2) Impairment of the root growth should be also observed if pH was the reason for the toxicity. However in our study only the growth of shoots was impaired. Therefore, the low pH itself is not the main driver of the toxicity. Instead,the GO induced decrease of pH can increase Fe mobilization and cause the observed Fe overload in the shoots.[39] Fig. 6B further showed that the Fe content flux in the xylem sap was significantly enhanced by GO treatment.

Considering the high capacity for absorption of GBMs which results from their high surface area, we further examined another possibility, which is that GO may enrich Fe on their surface by adsorption and then translocate to the leaves which may enhance the Fe uptake. To do so, we compared the adsorption of Fe on GO and rGO (see method in Section 1, SI). The amount of Fe adsorbed onto GO and rGO was 1.22 mg/L and 1.31 mg/L (Fig. 6C), respectively, which was nearly half of the Fe present in the nutrient solution (2.9 mg/L). We then estimated the amount

of Fe that can be translocated with the GO and rGO to the shoots (see method for estimation of uptake in Section 1, SI). Only 0.098 mg/kg of Fe can be attributed to transport into the plants *via* adsorption onto the GO or rGO. This is negligible compared with the total amount of Fe that was accumulated in the leaves (325 mg/kg), suggesting that the contribution of this mechanism to Fe overload is negligible.

When the pH of the GO suspension was adjusted back to normal pH (5.5) (see details of methods in SI), the phytotoxicity was eliminated (Fig. 6D and 6E) and the Fe content in shoots was normal (Fig. 6F). These results provide solid evidence that Fe overload is the main cause of the GO induced toxicity.

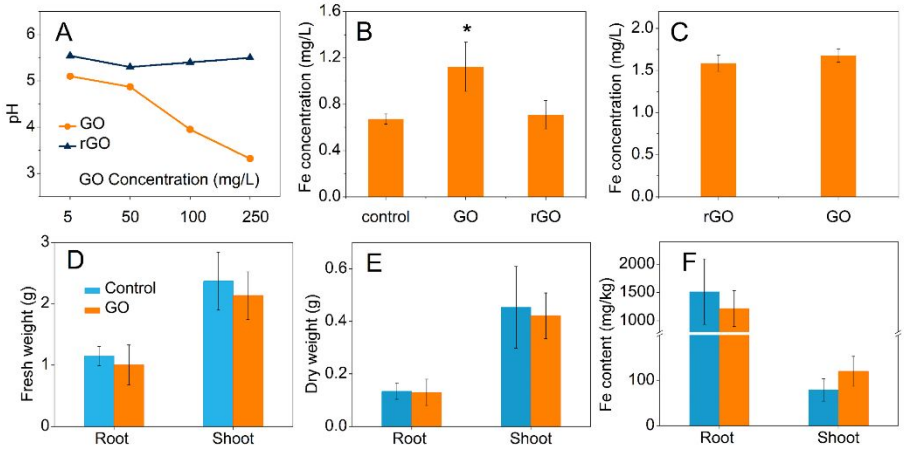

Fig. 6. pH values of GO and rGO suspensions in nutrient solution (A), the free Fe concentration in collected xylem saps (B), and the free Fe concentration in nutrient solution after incubation with GO and rGO (C) from a starting concentration of 2.9 mg/L. Fresh weight (D) and dry weight (E) of plant and Fe content (F) in plant after exposure to pH adjusted GO suspension (250 mg/L, pH 5.5) for 3 weeks. * indicates significant difference compared with control at $P < 0.05$.

3.7. Plant defence against Fe overload via reduced production of Fe transport associated metabolites

In our study, we found depressed production or excretion of iron-mobilizing coumarin-type compounds and iron-chelating flavonoid-type compounds (Fig. 7) in the leaves of GO treated plants, which may act as an important component of the iron depletion strategy in response to

Fe overload. Coumarin-derived phenolics or their corresponding glycosides were all dramatically depressed in the GO treated plants. For example, psoralen, a linear furanocoumarin, was decreased by 36% (Fig. 7A). The coumaric acid ester, 3-hydroxycinnamic acid, and cinnamoylcholine (a cinnamic acid ester), which are intermediates in the coumarin biosynthetic pathway, were significantly decreased by 78%, 62%, and 60%, respectively. The glycosides, such as coumarin glycoside (4-methylumbelliferyl glucuronide) and cinnamoyl glycoside, were also significantly decreased. In addition, an array of flavonoid-derived compounds, including flavonoids (e.g. flavanones, flavones, flavonols, anthocyanidin), the methylated derivatives, and their glycosides were all downregulated in the GO exposed plants (Fig. 7B). For example, the concentrations of cyanidin (a type of anthocyanidin), kaempferol (a natural flavonol), naringenin (a flavanone), 6-hydroxyflavone (a flavone), and corymbosin (a flavone), were depressed by 70%, 66%, 48%, 56% and 44%, respectively. The decrement for other flavonoid derivatives ranged from 41% to 65%. These data suggest that regulatory mechanisms at the metabolic level were evoked in leaves in order to sustain the iron homeostasis in response to GO-induced Fe overload.

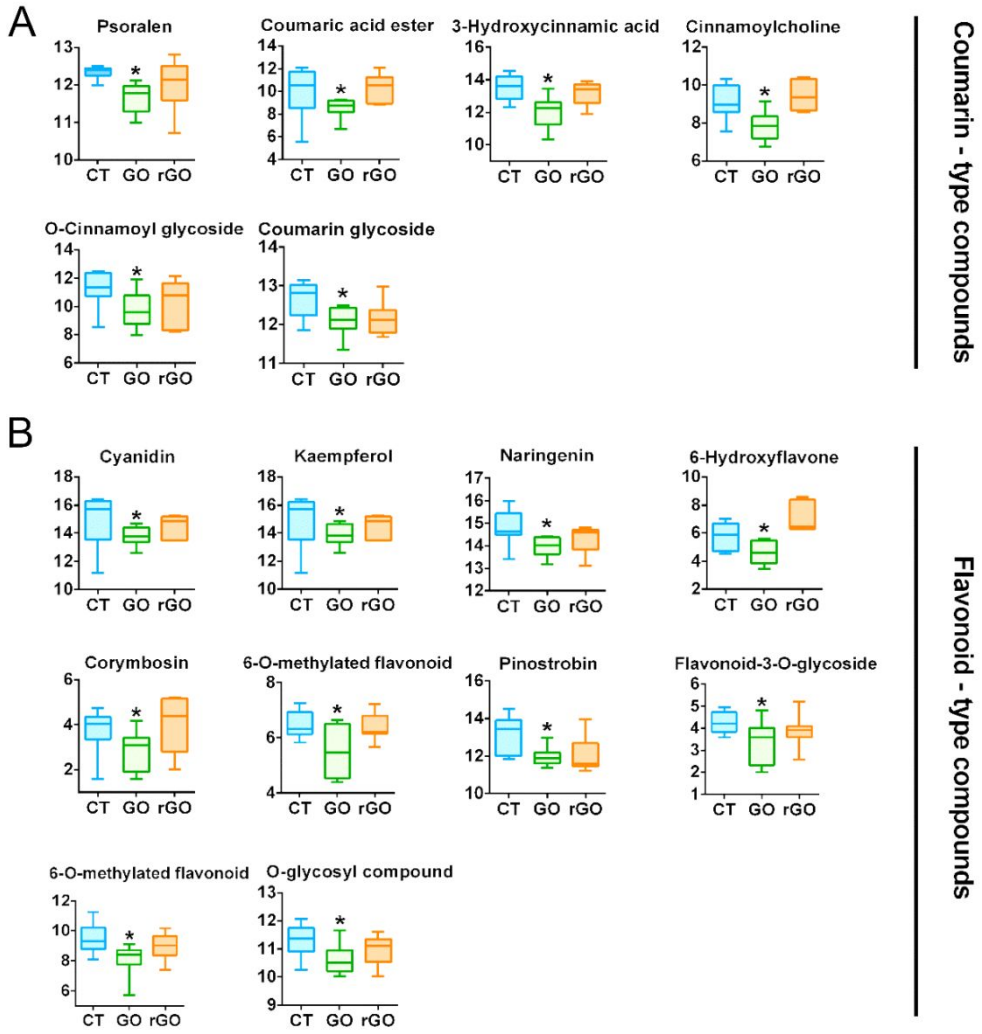

Fig. 7. Box plots of relative abundance of coumarin-type compounds (A) and flavonoid-type compounds (B) in the leaves of rice treated with 250 mg/L GO and rGO compared to the untreated controls (n=8). * indicates significant difference compared with control.

3.8. Biotransformation of GO as a pathway to alleviate GO-induced phytotoxicity

ENMs may transform by interaction with plants, the process of which may determine their subsequent behaviour, fate and toxicity in plants. CeO_2 ENMs are reported to be transformed in many plant species,[41, 42] being reduced and releasing Ce^{3+}, which is found to be responsible for the toxicity of CeO_2 ENMs to *Lactuca* plants.[42] The released Ce^{3+} can bind with phosphates, which could be a detoxification process.[43, 44] Transformation of graphene materials has been reported in bacteria,[28] plants[45] and in water under sunlight.[46] Free radicals (OH•) were

reported to be involved in the transformation of graphene into CO_2 in plant leaves, the process of which contributed to the elimination of graphene from plants following uptake and may thus reduce graphene induced phytotoxicity.[45] Immobilization of root exudates onto GO and formation of ligand-GO complexes were also reported, which decreased the surface charge and increased the unpaired electrons and the toxicity of the GO to zebrafish.[47]

We found that GO adsorbed onto the root surface, with a significant change of morphology from sheet to a folded shape (Fig. 8A and 8B). A root exudate (RE) layer between the GO and the root epidermis cells can be observed, which might act as a barrier to prevent the GO from entering the roots. Adsorption of GO onto the root surface was also clearly visible under the Raman microscope (Fig. 8C). The Id/Ig ratios (0.715-0.783) of the Raman spectra, collected from three spots on the roots (Figure 8D), were significantly lower than that of pristine GO (0.98, Fig. S7, Table S4), suggesting that roots enhanced the disorder in the structure of GO.[47] The O/C ratios of GO decreased significantly after interaction with plants (Fig. 8E and 8F, Table S4), suggesting the partial transformation of GO into rGO. GO-W (which were washed from the root surface) showed a higher reduction degree (O/C, 0.31) than GO-R (O/C, 0.4), suggesting that direct contact with the plant roots accelerated the reduction of GO. XRD analysis further confirmed the transformation of GO into rGO (Fig. 8G). Incubation in nutrient solution (GO-N) only induced a slight shift of the (002) peak of GO from 11.6° to 12.3°, suggesting no alteration of the crystal structure but a decrease of the lattice spacing. However, interaction of GO with roots (GO-W) not only induced a shift of the (002) peak to 9.7° but also led to the formation of a new peak at 28.6° which is attributed to the (002) peak of rGO, suggesting the reduction of GO.[48] In agreement with the XPS and XRD results, FTIR showed that GO-W was reduced to a higher degree than GO-R, suggesting that contact of GO with plant roots facilitated the transformation of GO to rGO (Fig. 8H). The transformation of "toxic" GO into a relatively low-toxic "rGO" might act as a pathway to alleviate the toxicity of GO. The potential role of root-associated microbes in the transformation process remains to be explored.

Adsorption of rGO onto the root surface was also observed by TEM (Fig. S9). FTIR spectra (Fig. S10) showed increased intensity of surface oxygen content after interaction with plant

418 roots (rGO-W), suggesting partial oxidation of rGO. However, XRD analysis showed that the
419 main peak (002) of rGO has not shifted (Fig. S11), suggesting no changes to the crystal structure.
420 The increased surface oxygen content observed by FTIR might be due to the adsorption of
421 organic compounds from root exudates.

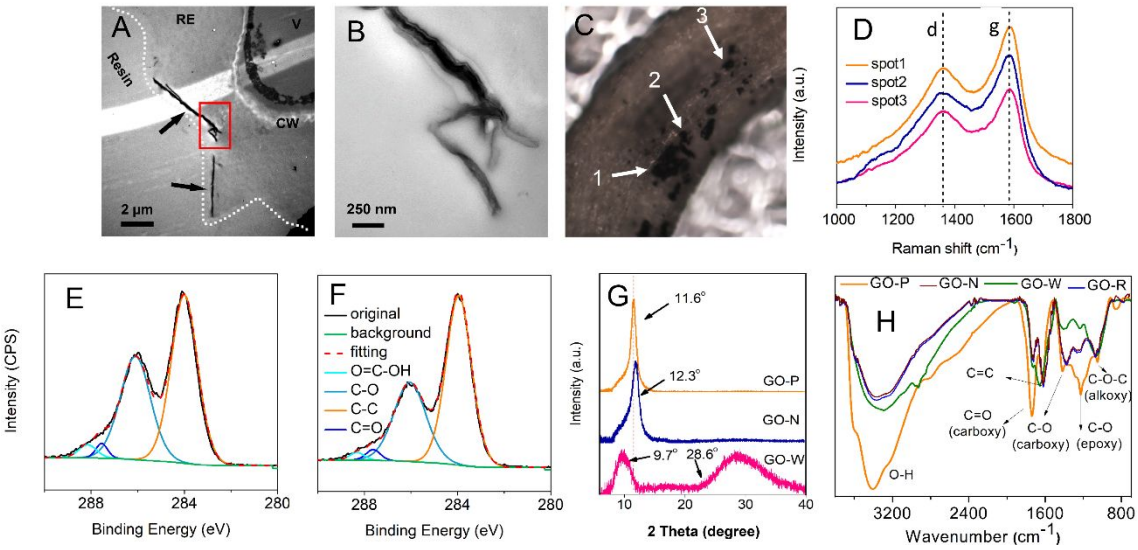

422

423 **Fig. 8.** Characterization of GO after interaction with plants for 3 weeks. (A and B) TEM images
424 of root sections; B is the magnified image of the rectangle area shown in A. RE indicates the root
425 exudate, CW indicates the cell wall. (C) Optical image of roots. (D) Raman spectra collected at
426 the three spots shown in C; d and g indicate the d band at 1363 cm^{-1} and g band at 1593 cm^{-1},
427 respectively. The intensity ratios of d to g, i.e. Id/Ig ratios, were 0.715 (spot 1), 0.723 (spot 2)
428 and 0.783 (spot 3), respectively. (E) XPS spectra of GO-R (GO in residual NS after removal of
429 plants). (F) Raman spectra of GO-W (GO washed off from roots). (G) XRD spectra of GO-P
430 (pristine GO), GO-N (GO incubated in nutrient solution for 3 weeks) and GO-W. (H) FTIR spectra
431 of GO-P, GO-N, GO-W and GO-R.

432

433 The present study reports for the first time a new mechanism of ENM induced phytotoxicity,
434 i.e. GO induced pH alteration of nutrient solution and subsequent Fe over accumulation and
435 oxidative damage in plant leaves. Some previous studies have suggested that ENMs can disturb
436 the macro and micro element distribution in plants, however, a clear interpretation of these
437 findings are lacking. The present study indicates that ENMs may cause toxicity to plants

indirectly by altering the micronutrient uptake. The apparently different impact of GO and rGO on plant growth suggests that the phytotoxicity of GBMs is highly related to their surface oxygen content. The inconsistent use of GO or rGO with different surface oxygen densities might be one of the reasons that explain the inconsistence in current literature. It should be noted that this is a short term study carried out in hydroponic condition. Effects of GBMs on plant in realistic soil environment over longer exposure time might be different and the mechanisms involved will be complicated by the soil components, which requires further studies.

ASSOCIATED CONTENT

The Supporting Information is available free of charge on the ACS Publications website. It includes additional experimental details and results.

AUTHOR INFORMATION

Corresponding authors

Email: p.zhang.1@bham.ac.uk (P. Zhang); zhangzhy@ihep.ac.cn (Z.Y. Zhang)

ACKNOWLEDGEMENT

This work was supported by Marie Skłodowska-Curie Individual Fellowships (NanoLabels Grant Agreement No. 750455 to PZ; NanoBBB Grant Agreement No. 798505 to ZG) under the European Union's Horizon 2020 research program.

CONFLICT OF INTEREST

The authors declare no conflict of interest.

REFERENCES

1. Geim, A. K., Graphene: status and prospects. *Science* **2009,** *324*, 1530-1534.
2. Avouris, P., Graphene: electronic and photonic properties and devices. *Nano Lett.* **2010,** *10*, 4285-4294.
3. Tonelli, F. M.; Goulart, V. A.; Gomes, K. N.; Ladeira, M. S.; Santos, A. K.; Lorençon, E.; Ladeira, L. O.; Resende, R. R., Graphene-based nanomaterials: biological and medical applications and toxicity. *Nanomedicine* **2015,** *10*, 2423-2450.
4. Chabot, V.; Higgins, D.; Yu, A.; Xiao, X.; Chen, Z.; Zhang, J., A review of graphene and graphene oxide sponge: material synthesis and applications to energy and the environment. *Energy*

Environ. Sci. **2014,** *7*, 1564-1596.
5. Zhao, J.; Wang, Z.; White, J. C.; Xing, B., Graphene in the aquatic environment: adsorption, dispersion, toxicity and transformation. *Environ. Sci. Technol.* **2014,** *48*, 9995-10009.
6. Sanchez, V. C.; Jachak, A.; Hurt, R. H.; Kane, A. B., Biological interactions of graphene-family nanomaterials: an interdisciplinary review. *Chem. Res. Toxicol.* **2011,** *25*, 15-34.
7. Gurunathan, S.; Arsalan Iqbal, M.; Qasim, M.; Park, C. H.; Yoo, H.; Hwang, J. H.; Uhm, S. J.; Song, H.; Park, C.; Do, J. T., Evaluation of Graphene Oxide Induced Cellular Toxicity and Transcriptome Analysis in Human Embryonic Kidney Cells. *Nanomaterials* **2019,** *9*, 969.
8. Wang, Q.; Li, C.; Wang, Y.; Que, X., Phytotoxicity of Graphene Family Nanomaterials and Its Mechanisms: A Review. *Frontiers in chemistry* **2019,** *7*.
9. Kabiri, S.; Degryse, F.; Tran, D. N.; da Silva, R. C.; McLaughlin, M. J.; Losic, D., Graphene Oxide: A New Carrier for Slow Release of Plant Micronutrients. *ACS applied materials & interfaces* **2017,** *9*, 43325-43335.
10. Zhang, M.; Gao, B.; Chen, J.; Li, Y.; Creamer, A. E.; Chen, H., Slow-release fertilizer encapsulated by graphene oxide films. *Chem. Eng. J.* **2014,** *255*, 107-113.
11. Andelkovic, I. B.; Kabiri, S.; Tavakkoli, E.; Kirby, J. K.; McLaughlin, M. J.; Losic, D., Graphene oxide-Fe (III) composite containing phosphate–A novel slow release fertilizer for improved agriculture management. *Journal of cleaner production* **2018,** *185*, 97-104.
12. Ren, W.; Ren, G.; Teng, Y.; Li, Z.; Li, L., Time-dependent effect of graphene on the structure, abundance, and function of the soil bacterial community. *J. Hazard. Mater.* **2015,** *297*, 286-294.
13. Chung, H.; Kim, M. J.; Ko, K.; Kim, J. H.; Kwon, H.-a.; Hong, I.; Park, N.; Lee, S.-W.; Kim, W., Effects of graphene oxides on soil enzyme activity and microbial biomass. *Sci. Total Environ.* **2015,** *514*, 307-313.
14. Kim, M.-J.; Ko, D.; Ko, K.; Kim, D.; Lee, J.-Y.; Woo, S. M.; Kim, W.; Chung, H., Effects of silver-graphene oxide nanocomposites on soil microbial communities. *J. Hazard. Mater.* **2018,** *346*, 93-102.
15. Dong, S.; Xia, T.; Yang, Y.; Lin, S.; Mao, L., Bioaccumulation of 14C-labeled graphene in an aquatic food chain through direct uptake or trophic transfer. *Environ. Sci. Technol.* **2018,** *52*, 541-549.
16. Begum, P.; Ikhtiari, R.; Fugetsu, B., Graphene phytotoxicity in the seedling stage of cabbage, tomato, red spinach, and lettuce. *Carbon* **2011,** *49*, 3907-3919.
17. Zhang, P.; Zhang, R.; Fang, X.; Song, T.; Cai, X.; Liu, H.; Du, S., Toxic effects of graphene on the growth and nutritional levels of wheat (Triticum aestivum L.): short-and long-term exposure studies. *J. Hazard. Mater.* **2016,** *317*, 543-551.
18. Cheng, F.; Liu, Y.-F.; Lu, G.-Y.; Zhang, X.-K.; Xie, L.-L.; Yuan, C.-F.; Xu, B.-B., Graphene oxide modulates root growth of Brassica napus L. and regulates ABA and IAA concentration. *J. Plant Physiol.* **2016,** *193*, 57-63.
19. Chen, L.; Wang, C.; Li, H.; Qu, X.; Yang, S.-T.; Chang, X.-L., Bioaccumulation and toxicity of 13C-skeleton labeled graphene oxide in wheat. *Environ. Sci. Technol.* **2017,** *51*, 10146-10153.
20. Zhou, Q.; Hu, X., Systemic stress and recovery patterns of rice roots in response to graphene oxide nanosheets. *Environ. Sci. Technol.* **2017,** *51*, 2022-2030.
21. Servin, A. D.; White, J. C., Nanotechnology in agriculture: next steps for understanding engineered nanoparticle exposure and risk. *NanoImpact* **2016,** *1*, 9-12.

22. Hu, X.; Zhou, Q., Novel hydrated graphene ribbon unexpectedly promotes aged seed germination and root differentiation. *Sci. Rep.* **2014,** *4*, 3782.
23. He, Y.; Hu, R.; Zhong, Y.; Zhao, X.; Chen, Q.; Zhu, H., Graphene oxide as a water transporter promoting germination of plants in soil. *Nano Research* **2018,** *11*, 1928-1937.
24. Zhang, P.; Ma, Y.; Xie, C.; Guo, Z.; He, X.; Valsami-Jones, E.; Lynch, I.; Luo, W.; Zheng, L.; Zhang, Z., Plant species-dependent transformation and translocation of ceria nanoparticles. *Environmental Science: Nano* **2019,** *6*, 60-67.
25. Wang, Q.; Zhao, S.; Zhao, Y.; Rui, Q.; Wang, D., Toxicity and translocation of graphene oxide in Arabidopsis plants under stress conditions. *RSC Advances* **2014,** *4*, 60891-60901.
26. Cui, D.; Zhang, P.; Ma, Y.; He, X.; Li, Y.; Zhang, J.; Zhao, Y.; Zhang, Z., Effect of cerium oxide nanoparticles on asparagus lettuce cultured in an agar medium. *Environmental Science: Nano* **2014,** *1*, 459-465.
27. De Jesus, L. R.; Dennis, R. V.; Depner, S. W.; Jaye, C.; Fischer, D. A.; Banerjee, S. J. T. j. o. p. c. l., Inside and outside: X-ray absorption spectroscopy mapping of chemical domains in graphene oxide. **2013,** *4*, 3144-3151.
28. Guo, Z.; Xie, C.; Zhang, P.; Zhang, J.; Wang, G.; He, X.; Ma, Y.; Zhao, B.; Zhang, Z., Toxicity and transformation of graphene oxide and reduced graphene oxide in bacteria biofilm. *Sci. Total Environ.* **2017,** *580*, 1300-1308.
29. Liu, L.; Zhu, C.; Fan, M.; Chen, C.; Huang, Y.; Hao, Q.; Yang, J.; Wang, H.; Sun, D., Oxidation and degradation of graphitic materials by naphthalene-degrading bacteria. *Nanoscale* **2015,** *7*, 13619-13628.
30. Zhang, P.; He, X.; Ma, Y.; Lu, K.; Zhao, Y.; Zhang, Z., Distribution and bioavailability of ceria nanoparticles in an aquatic ecosystem model. *Chemosphere* **2012,** *89*, 530-535.
31. Wang, J.; Wei, Y.; Shi, X.; Gao, H., Cellular entry of graphene nanosheets: the role of thickness, oxidation and surface adsorption. *Rsc Advances* **2013,** *3*, 15776-15782.
32. Ren, W.; Chang, H.; Teng, Y., Sulfonated graphene-induced hormesis is mediated through oxidative stress in the roots of maize seedlings. *Sci. Total Environ.* **2016,** *572*, 926-934.
33. Mahender, A.; Swamy, B.; Anandan, A.; Ali, J., Tolerance of iron-deficient and-toxic soil conditions in rice. *Plants* **2019,** *8*, 31.
34. Kehrer, J. P., The Haber–Weiss reaction and mechanisms of toxicity. *Toxicology* **2000,** *149*, 43-50.
35. Shane, M. W.; McCully, M. E.; Lambers, H., Tissue and cellular phosphorus storage during development of phosphorus toxicity in Hakea prostrata (Proteaceae). *J. Exp. Bot.* **2004,** *55*, 1033-1044.
36. Müller, C.; Kuki, K. N.; Pinheiro, D. T.; de Souza, L. R.; Silva, A. I. S.; Loureiro, M. E.; Oliva, M. A.; Almeida, A. M., Differential physiological responses in rice upon exposure to excess distinct iron forms. *Plant Soil* **2015,** *391*, 123-138.
37. Zhang, P.; Ma, Y.; Zhang, Z., Interactions between engineered nanomaterials and plants: phytotoxicity, uptake, translocation, and biotransformation. In *Nanotechnology and Plant Sciences*, Springer: 2015; pp 77-99.
38. Liu, S.; Zeng, T. H.; Hofmann, M.; Burcombe, E.; Wei, J.; Jiang, R.; Kong, J.; Chen, Y., Antibacterial activity of graphite, graphite oxide, graphene oxide, and reduced graphene oxide: membrane and oxidative stress. *ACS nano* **2011,** *5*, 6971-6980.

553 39. Zhao, T.; LING, H. Q., Effects of pH and nitrogen forms on expression profiles of genes
554 involved in iron homeostasis in tomato. *Plant, Cell Environ.* **2007,** *30*, 518-527.
555 40. Tanaka, A.; Navasero, S., Growth of the rice plant on acid sulfate soils. *Soil Sci. Plant Nutr.*
556 **1966,** *12*, 23-30.
557 41. Zhang, P.; Ma, Y.; Zhang, Z.; He, X.; Zhang, J.; Guo, Z.; Tai, R.; Zhao, Y.; Chai, Z.,
558 Biotransformation of ceria nanoparticles in cucumber plants. *ACS nano* **2012,** *6*, 9943-9950.
559 42. Zhang, P.; Ma, Y.; Zhang, Z.; He, X.; Li, Y.; Zhang, J.; Zheng, L.; Zhao, Y., Species-specific toxicity
560 of ceria nanoparticles to Lactuca plants. *Nanotoxicology* **2015,** *9*, 1-8.
561 43. Li, R.; Ji, Z.; Chang, C. H.; Dunphy, D. R.; Cai, X.; Meng, H.; Zhang, H.; Sun, B.; Wang, X.; Dong,
562 J., Surface interactions with compartmentalized cellular phosphates explain rare earth oxide
563 nanoparticle hazard and provide opportunities for safer design. *ACS nano* **2014,** *8*, 1771-1783.
564 44. Briffa, S. M.; Lynch, I.; Hapiuk, D.; Valsami-Jones, E., Physical and chemical transformations
565 of zirconium doped ceria nanoparticles in the presence of phosphate: Increasing realism in
566 environmental fate and behaviour experiments. *Environ. Pollut.* **2019**.
567 45. Huang, C.; Xia, T.; Niu, J.; Yang, Y.; Lin, S.; Wang, X.; Yang, G.; Mao, L.; Xing, B., Transformation
568 of 14C-Labeled Graphene to 14CO2 in the Shoots of a Rice Plant. *Angew. Chem.* **2018,** *130*, 9907-
569 9911.
570 46. Hou, W.-C.; Chowdhury, I.; Goodwin Jr, D. G.; Henderson, W. M.; Fairbrother, D. H.; Bouchard,
571 D.; Zepp, R. G., Photochemical transformation of graphene oxide in sunlight. *Environ. Sci.*
572 *Technol.* **2015,** *49*, 3435-3443.
573 47. Du, J.; Hu, X.; Mu, L.; Ouyang, S.; Ren, C.; Du, Y.; Zhou, Q., Root exudates as natural ligands
574 that alter the properties of graphene oxide and environmental implications thereof. *Rsc*
575 *Advances* **2015,** *5*, 17615-17622.
576 48. Huang, H.-H.; De Silva, K. K. H.; Kumara, G.; Yoshimura, M., Structural evolution of
577 hydrothermally derived reduced graphene oxide. *Sci. Rep.* **2018,** *8*, 6849.
578